Examples of Bivariate Non-separable Compactly Supported Orthonormal Continuous Wavelets

Wenjie He and Ming-Jun Lai
Department of Mathematics, University of Georgia, Athens, GA 30602, USA
mjlai@math.uga.edu.

ABSTRACT

We give several examples of bivariate non-separable compactly supported orthonormal wavelets whose scaling functions are supported over [0,3]x[0,3]. The Hölder continuity properties of these wavelets are studied.

Keywords: Non-separable, Compact support, Orthonormal, Continuous, Wavelet

1. INTRODUCTION

Univariate wavelets have found successful applications in signal processing since wavelet expansions are more appropriate than conventional Fourier series to represent the abrupt changes in non-stationary signals. To apply wavelet methods to digital image processing, we have to construct bivariate wavelets. The most commonly used method is the tensor product of univariate wavelets. This construction leads to a separable wavelet which has a disadvantage of giving a particular importance to the horizontal and vertical directions. Much effort has been spent on constructing non-separable bivariate wavelets. For example, in [1], Riemenschneider and Shen used bivariate box splines which are natural generalizations of B-splines to construct wavelets. These wavelets have infinite support, like the Battle-Lemarié wavelets. References [2], [3], [4], and [5] also discuss non-separable compactly supported biorthogonal wavelets and prewavelets. In [6], Cohen and Daubechies generalized the method in [7] to constructed non-separable bidimensional (discontinuous) compactly supported wavelets. Also, in [8], Kovačević and Vetterli studied properties of multidimensional non-separable wavelets and numerically constructed examples of continuous non-separable compactly supported bivariate wavelets. Both Cohen-Daubechies' wavelets and Kovačević-Vetterli's examples are based on the dilation matrix $\begin{bmatrix} 1 & 1 \\ 1 & -1 \end{bmatrix}$. In this paper, we construct bivariate non-separable compactly supported orthonormal wavelets based on the commonly used uniform dilation matrix $\begin{bmatrix} 2 & 0 \\ 0 & 2 \end{bmatrix}$.

To construct these wavelets, we start by constructing a compactly supported scaling function ϕ which generates multi-resolution analysis of $L_2(\mathbf{R}^2)$. Let

$$m_0(\omega) := m_0(\omega_1, \omega_2) = \sum_{0 \le j \le p, 0 \le k \le q} c_{j,k} \exp(i(j\omega_1 + k\omega_2))$$

be a bivariate trigonometric polynomial. We will construct m_0 which satisfies the following requirements:

1°. $m_0(0,0) = 1$;

2°. $\sum_{j=0}^{3} |m_0(\omega+\pi_j)|^2 = 1$ with $\pi_0=(0,0)$, $\pi_1=(\pi,0)$, $\pi_2=(0,\pi)$, and $\pi_3=(\pi,\pi)$.

Let $\hat{\phi}(\omega) = \prod_{k=1}^{\infty} m_0(\omega/2^k)$. Then 1° implies the convergence of this infinite product and hence $\hat{\phi}$ is a well defined continuous function. 2° implies $\hat{\phi} \in L_2(\mathbf{R}^2)$. Thus, $\phi \in L_2(\mathbf{R}^2)$ by Plancheral's Theorem. For a fixed ordering which maps bi-integers $(0,0) \le (j,k) \le (p,q)$ into positive integers $\{1,2,\ldots,N\}$ with $N=(p+1)(q+1)$, let A be a matrix of size $N \times N$ with entries

$$A_{k_1,k_2;\ell_1,\ell_2} = 4 \sum_{j_1,j_2} c_{j_1,j_2}\, \overline{c_{(j_1,j_2)+(k_1,k_2)-2(\ell_1,\ell_2)}},$$

for $(0,0) \le (k_1,k_2),(\ell_1,\ell_2) \le (p,q)$. In order to make $\{\phi(x-k_1,y-k_2),(k_1,k_2)\in Z^2\}$ an orthonormal set, we need to have

3°. 1 is a non-degenerate eigenvalue of A.

We then further study the coefficients of m_0 such that $\phi \in C(\mathbf{R}^2)$ and other higher order regularities, i.e.,

4°. $\phi \in C^{\gamma}(\mathbf{R}^2)$ with $\gamma \ge 0$.

After these preparations, we shall construct m_ν, $\nu=1,2,3$, such that

5°. $\sum_{j=0}^{3} m_\mu(\omega+\pi_j)\overline{m_\nu(\omega+\pi_j)} = \delta_{\mu,\nu}, \quad \mu,\nu = 0,1,2,3.$

To make m_0 to be a low-pass filter, we require that m_0 have a factor $(1+e^{i\omega})(1+e^{i\omega_2})$. Thus, m_0 satisfies the following

6°. $m_0(\pi,\omega_2) = 0 = m_0(\omega_1,\pi)$ for all $(\omega_1,\omega_2) \in [-\pi,\pi]$.

For $p=q=3$, we are able to give the complete solution set of all m_0 satisfying 1°, 2°, and 6°. We are able to identify many sets of solutions which further satisfy 3° and 4°. In particular, any tensor product of two univariate scaling functions with support in [0,3] is in our solution sets (Example 2.1). For instance, a tensor product of Daubechies' scaling function ${}_2\phi$ is included. It is known that ${}_2\phi(x_1){}_2\phi(x_2) \in C^{\alpha}(\mathbf{R}^2)$ with $\alpha \ge 0.5$ [9]. We can expect other solutions to have certain Hölder's exponents. We also find linear phase filters which generate an orthonormal scaling function (Example 2.2). There are infinitely many filters m_0 which are symmetric in the sense that $c_{k_1,k_2} = c_{k_2,k_1}$ (Example 2.3). Also, there are infinitely many filters m_0 which are neither linear phase nor symmetric with respect to the line $x=y$ (Example 2.4). We study the regularity of those filters. Finally, we give two methods of construction of m_ν. One is for linear phase filters m_0 and the other is for any given m_0 satisfying 1° and 2°. Once we have m_ν, we define

$$\hat{\psi}_\mu(\omega) = m_\mu(\omega/2)\,\hat{\phi}(\omega/2), \quad \mu=1,2,3.$$

These ψ_ν will be the non-separable compactly supported orthonormal wavelets.

These constructions are given in Section 2. In Section 3, we present some numerical experiments using our non-separable wavelets which show that the high frequency bands by non-separable wavelets reveal more features than by separable wavelets. This may find applications in pattern recognition, texture analysis and edge detection. Also, we present a comparison of image compressions using tensor product and non-separable wavelets. We show that for text images, our non-separable wavelets do a better job.

2. CONSTRUCTION OF SCALING FUNCTIONS AND WAVELETS

Rewrite $m_0(\omega_1, \omega_2)$ as

$$m(x, y) = \sum_{0 \le j \le p, 0 \le k \le q} c_{j,k} x^j y^k$$

with $x = e^{i\omega_1}$ and $y = e^{i\omega_2}$. Also write $m(x, y)$ in its polyphase form:

$$m(x, y) = f_0(x^2, y^2) + x f_1(x^2, y^2) + y f_2(x^2, y^2) + xy f_3(x^2, y^2). \tag{1}$$

The requirement 2° is equivalent to

$$|m(x, y)|^2 + |m(-x, y)|^2 + |m(x, -y)|^2 + |m(-x, -y)|^2 = 1, \quad \forall |x| = |y| = 1. \tag{2}$$

We have the following elementary lemma.

Lemma 2.1. *A polynomial m satisfies (2) if and only if its polyphase components f_0, f_1, f_2, f_3 satisfy*

$$|f_0|^2 + |f_1|^2 + |f_2|^2 + |f_3|^2 = \frac{1}{4}. \tag{3}$$

From now on, we only consider $p = q = 3$. Thus, we write

$$f_\nu(x, y) = a_\nu + b_\nu x + c_\nu y + d_\nu xy, \quad \nu = 0, 1, 2, 3. \tag{4}$$

The requirement 1° implies $m(1, 1) = 1$, i.e.,

$$\sum_{\nu=0}^{3} a_\nu + b_\nu + c_\nu + d_\nu = 1. \tag{5}$$

In addition, the requirement 6° implies $m(-1, y) = 0 = m(x, -1)$ and hence,

$$a_\nu + b_\nu + c_\nu + d_\nu = \frac{1}{4}, \quad \nu = 0, 1, 2, 3. \tag{6}$$

Lemma 2.2. *f_0, f_1, f_2 and f_3 satisfy (3) if and only if*

$$\sum_{\nu=0}^{3} (a_\nu b_\nu + c_\nu d_\nu) = 0, \quad \sum_{\nu=0}^{3} (a_\nu c_\nu + b_\nu d_\nu) = 0, \tag{7}$$

$$\sum_{\nu=0}^{3} a_\nu d_\nu = 0, \quad \sum_{\nu=0}^{3} b_\nu c_\nu = 0, \tag{8}$$

and

$$\sum_{\nu=0}^{3} (a_\nu^2 + b_\nu^2 + c_\nu^2 + d_\nu^2) = \frac{1}{4}. \tag{9}$$

This may be verified by straightforward calculation. We now present one of the main results in this paper.

Theorem 2.1. *Let*

$$\begin{aligned} m(x,y) = \sum_{0\le j\le 3, 0\le k\le 3} c_{j,k} x^j y^k &= \frac{(1+x)(1+y)}{16}(a_{00} + a_{10}x + a_{01}y + a_{11}xy \\ &\quad + a_{20}x^2 + a_{21}x^2 y + a_{12}xy^2 + a_{22}x^2y^2 + a_{02}y^2) \end{aligned} \tag{10}$$

with

$$\begin{cases} a_{00} = 1 + \sqrt{2}(\cos\alpha + \cos\beta) + 2\cos\theta\cos\xi \\ a_{10} = \sqrt{2}(\sin\alpha - \cos\alpha) - 2\cos\theta\cos\xi + 2\cos\theta\sin\xi \\ a_{01} = \sqrt{2}(\sin\beta - \cos\beta) - 2\cos\theta\cos\xi + 2\sin\theta\cos\eta \\ a_{11} = 2(\cos\theta\cos\xi + \sin\theta\sin\eta - \cos\theta\sin\xi - \sin\theta\cos\eta) \\ a_{20} = 1 + \sqrt{2}(\cos\beta - \sin\alpha) - 2\cos\theta\sin\xi \\ a_{02} = 1 + \sqrt{2}(\cos\alpha - \sin\beta) - 2\sin\theta\cos\eta \\ a_{21} = \sqrt{2}(\sin\beta - \cos\beta) - 2\sin\theta\sin\eta + 2\cos\theta\sin\xi \\ a_{12} = \sqrt{2}(\sin\alpha - \cos\alpha) - 2\sin\theta\sin\eta + 2\sin\theta\cos\eta \\ a_{22} = 1 - \sqrt{2}(\sin\alpha + \sin\beta) + 2\sin\theta\sin\eta. \end{cases} \tag{11}$$

Suppose that $\alpha, \beta, \theta, \xi, \eta$ satisfy the following

$$\cos\theta\cos\xi + \cos\theta\sin\xi + \sin\theta\cos\eta + \sin\theta\sin\eta = 2\sin(\alpha + \frac{\pi}{4})\sin\left(\beta + \frac{\pi}{4}\right). \tag{12}$$

Then $m(x,y)$ satisfies (2).

Proof: It follows from (7), (8) and (9) that

$$\sum_{\nu=0}^{3} (a_\nu - b_\nu)^2 + (c_\nu - d_\nu)^2 = \frac{1}{4}$$

and

$$\sum_{\nu=0}^{3} (a_\nu - b_\nu)(c_\nu - d_\nu) = 0.$$

Then we have

$$\sum_{\nu=0}^{3} (a_\nu - b_\nu + c_\nu - d_\nu)^2 = \frac{1}{4}.$$

By (6), it follows that

$$\sum_{\nu=0}^{3} \left(2(a_\nu + c_\nu) - \frac{1}{4}\right)^2 = \frac{1}{4}.$$

Now $m(-1,y)=0=m(x,-1)$ implies that $a_0+c_0=a_2+c_2$ and $a_1+c_1=a_3+c_3$. It follows that

$$a_0+c_0=\frac{1}{8}+\frac{1}{4\sqrt{2}}\cos\alpha=a_2+c_2,\ \text{and}\ a_1+c_1=\frac{1}{8}+\frac{1}{4\sqrt{2}}\sin\alpha=a_3+a_3. \tag{13}$$

Similarly, we have

$$a_0+b_0=\frac{1}{8}+\frac{1}{4\sqrt{2}}\cos\beta=a_1+b_1\ \text{and}\ a_2+b_2=\frac{1}{8}+\frac{1}{4\sqrt{2}}\sin\beta=a_3+b_3. \tag{14}$$

In other words, we have

$$\begin{cases} b_i=\frac{1}{8}+\frac{1}{4\sqrt{2}}\cos\beta-a_i, & i=0,1,\\ b_i=\frac{1}{8}+\frac{1}{4\sqrt{2}}\sin\beta-a_i, & i=2,3,\\ c_i=\frac{1}{8}+\frac{1}{4\sqrt{2}}\cos\alpha-a_i, & i=0,2,\\ c_i=\frac{1}{8}+\frac{1}{4\sqrt{2}}\sin\alpha-a_i, & i=1,3,\\ d_0=-\frac{1}{4\sqrt{2}}(\cos\alpha+\cos\beta)+a_0,\\ d_1=-\frac{1}{4\sqrt{2}}(\sin\alpha+\cos\beta)+a_1,\\ d_2=-\frac{1}{4\sqrt{2}}(\cos\alpha+\sin\beta)+a_2,\\ d_3=-\frac{1}{4\sqrt{2}}(\sin\alpha+\sin\beta)+a_3. \end{cases} \tag{15}$$

We now find the relations among the a_ν's. By (8), specifically, $0=\sum_{\nu=0}^{3}a_\nu d_\nu$, we have

$$\begin{aligned} &\left(a_0-\frac{1}{8\sqrt{2}}(\cos\alpha+\cos\beta)\right)^2+\left(a_1-\frac{1}{8\sqrt{2}}(\sin\alpha+\cos\beta)\right)^2\\ &+\left(a_2-\frac{1}{8\sqrt{2}}(\cos\alpha+\sin\beta)\right)^2+\left(a_3-\frac{1}{8\sqrt{2}}(\sin\alpha+\sin\beta)\right)^2\\ =\ &\frac{1}{32}\left(1+\sin(\alpha+\frac{\pi}{4})\sin(\beta+\frac{\pi}{4})\right). \end{aligned} \tag{16}$$

By (8), specifically, $\sum_{\nu=0}^{3}b_\nu c_\nu=0$ and $\sum_{\nu=0}^{3}a_\nu d_\nu=0$, we have

$$\begin{aligned} &a_0-\frac{1}{8\sqrt{2}}(\cos\alpha+\cos\beta)+a_1-\frac{1}{8\sqrt{2}}(\sin\alpha+\cos\beta)\\ +\ &a_2-\frac{1}{8\sqrt{2}}(\cos\alpha+\sin\beta)+a_3-\frac{1}{8\sqrt{2}}(\sin\alpha+\sin\beta)\\ =\ &\frac{1}{4}\left(1+\sin(\alpha+\frac{\pi}{4})\sin(\beta+\frac{\pi}{4})\right). \end{aligned} \tag{17}$$

Let $\tilde{a}_0=a_0-\frac{1}{8\sqrt{2}}(\cos\alpha+\cos\beta)$, $\tilde{a}_1=a_1-\frac{1}{8\sqrt{2}}(\sin\alpha+\cos\beta)$, $\tilde{a}_2=a_2-\frac{1}{8\sqrt{2}}(\cos\alpha+\sin\beta)$, $\tilde{a}_3=a_3-\frac{1}{8\sqrt{2}}(\sin\alpha+\sin\beta)$. The equations (16) and (17) become

$$\left(\tilde{a}_0-\frac{1}{16}\right)^2+\left(\tilde{a}_1-\frac{1}{16}\right)^2+\left(\tilde{a}_2-\frac{1}{16}\right)^2+\left(\tilde{a}_3-\frac{1}{16}\right)^2=\left(\frac{1}{8}\right)^2.$$

It follows that

$$\begin{cases} a_0=\frac{1}{16}+\frac{1}{8\sqrt{2}}(\cos\alpha+\cos\beta)+\frac{1}{8}\cos\theta\cos\xi,\\ a_1=\frac{1}{16}+\frac{1}{8\sqrt{2}}(\sin\alpha+\cos\beta)+\frac{1}{8}\cos\theta\sin\xi,\\ a_2=\frac{1}{16}+\frac{1}{8\sqrt{2}}(\cos\alpha+\sin\beta)+\frac{1}{8}\sin\theta\cos\eta,\\ a_3=\frac{1}{16}+\frac{1}{8\sqrt{2}}(\sin\alpha+\sin\beta)+\frac{1}{8}\sin\theta\sin\eta. \end{cases} \tag{18}$$

By (17) and (18), $\alpha, \beta, \theta, \xi, \eta$ must satisfy

$$\begin{aligned} \frac{1}{4} &+ \frac{1}{8}(\cos\theta\cos\xi + \cos\theta\sin\xi + \sin\theta\cos\eta + \sin\theta\sin\eta) \\ &= \frac{1}{4} + \frac{1}{4}\sin\left(\alpha + \frac{\pi}{4}\right)\sin\left(\beta + \frac{\pi}{4}\right). \end{aligned}$$

After simplified, the above equation is (12). The above derivations show that any solution $m(x, y)$ satisfying $1°, 2°$, and $6°$ must be in the form (10) and (11) with $\alpha, \beta, \gamma, \xi, \eta$ satisfying (12).

On the other hand, any solution m in the form (10) and (11) with $\alpha, \beta, \gamma, \xi, \eta$ satisfying (12) will satisfy (17) and (16). These equations (17) and (16) are equivalent to $\sum_{\nu=0}^{3} a_\nu d_\nu = 0$ and $\sum_{\nu=0}^{3} b_\nu c_\nu = 0$. By the expressions (11), we have (13), (14) and (15). These equations imply that

$$\begin{aligned} \sum_{\nu=0}^{3}(a_\nu - b_\nu + c_\nu - d_\nu)^2 &= \frac{1}{4}, \\ \sum_{\nu=0}^{3}(a_\nu - b_\nu - c_\nu + d_\nu)^2 &= \frac{1}{4}, \\ \sum_{\nu=0}^{3}(a_\nu + b_\nu + c_\nu + d_\nu)^2 &= \frac{1}{4}. \end{aligned}$$

The above three equations are equivalent to the two equations in (7) and equation (9). This completes the proof. ■

Let us give several examples of filters $m(x, y)$ before studying their orthonormality conditions, regularity, and the construction of wavelets from the scaling functions generated by these filters.

Example 2.1. We first look for separable filters. If we set $\xi = \eta$ in (12), then (12) becomes

$$(\cos\theta + \sin\theta)(\cos\xi + \sin\xi) = (\cos\alpha + \sin\alpha)(\cos\beta + \sin\beta).$$

If we further choose $\theta = \beta$, then $\xi = \alpha$ and $m(x, y)$ in (10) may be simplified into

$$m(x, y) = M(x, \beta)M(y, \alpha)$$

with

$$M(x, \alpha) = \frac{1 + x}{4}(1 + \sqrt{2}\cos\alpha + \sqrt{2}(\sin\alpha - \cos\alpha)x + (1 - \sqrt{2}\sin\alpha)x^2). \tag{19}$$

Let

$$\hat{\phi}(\omega_1, \omega_2) = \prod_{k=1}^{\infty} M(e^{i\frac{\omega_1}{2^k}}, \alpha)M(e^{i\frac{\omega_2}{2^k}}, \beta)$$

be a scaling function, where α and β are some appropriate parameters. For $\alpha = \beta = \frac{5\pi}{12}$,

$$M(e^{i\omega}, 5\pi/12) = \frac{1}{2}\left[\frac{1 + \sqrt{3}}{4} + \frac{3 + \sqrt{3}}{4}e^{i\omega} + \frac{3 - \sqrt{3}}{4}e^{i2\omega} + \frac{1 - \sqrt{3}}{4}e^{i3\omega}\right]$$

is the filter associated with Daubechies' scaling function ${}_2\phi$ [9]. In this case, $\hat{\phi}(\omega_1,\omega_2) = {}_2\hat{\phi}(\omega_1)\ {}_2\hat{\phi}(\omega_2)$ which is a tensor product of the univariate scaling function.

Hence, for $\theta = \beta$ and $\xi = \eta = \alpha$, (12) is satisfied and $m(x,y)$ given in (10) is a separable filter.

■

Example 2.2. Let us look for linear phase filters. That is, we need to have

$$a_{00} = a_{22}, a_{02} = a_{20}, a_{12} = a_{10}, a_{01} = a_{21}.$$

Solving these four equations together with (12), we obtain the following 8 filters satisfying $1°, 2°$, and $6°$ with a fixed length $p = q = 3$ up to a shift.

$$1)\ m(x,y) = \frac{(1+x)(1+y)}{8}(-1+2x-x^2+2y-2xy+2x^2y-y^2+2xy^2-x^2y^2);$$

$$2)\ m(x,y) = \frac{(1+x)(1+y)}{8}(1+x^2-2y+2xy-2x^2y+y^2+x^2y^2);$$

$$3)\ m(x,y) = \frac{(1+x)(1+y)}{8}(1-2x+x^2+2xy+y^2-2xy^2+x^2y^2);$$

$$4)\ m(x,y) = \frac{x(1+x)(1+y)y}{4};$$

$$5)\ m(x,y) = \frac{(1+x)(1+y)}{8}(1+x^2-2xy+y^2+x^2y^2);$$

$$6)\ m(x,y) = \frac{(1+x^3)y(1+y)}{4};$$

$$7)\ m(x,y) = \frac{x(1+x)(1+y^3)}{4};$$

$$8)\ m(x,y) = \frac{(1+x^3)(1+y^3)}{4}.$$

Example 2.3. Let us consider the filter $m(x,y)$ symmetric with respect to the line $x = y$. Then $a_{12} = a_{21}, a_{02} = a_{20}, a_{01} = a_{10}$. These imply $\alpha = \beta$ and $\sin\theta\cos\eta = \cos\theta\sin\xi$. Then by (12), our $\alpha, \beta, \theta, \xi, \eta$, must satisfy

$$\begin{cases} \cos\theta\cos\xi \quad +2\cos\theta\sin\xi + \sin\theta\sin\eta = 2\sin^2\left(\alpha+\frac{\pi}{4}\right), \\ \qquad\qquad\qquad\quad \sin\theta\cos\eta = \cos\theta\sin\xi. \end{cases} \tag{20}$$

There are infinitely many possible ξ and η for which we can find θ and α satisfying the two equations in (20), including $(\xi,\eta) \in [\pi/10, 9\pi/10] \times [\pi/3, 19\pi/36]$. We list four concrete examples.

	Ex.2.3.1.	Ex.2.3.2.	Ex.2.3.3.	Ex.2.3.4
a_{00}	1.6330	2.1222	1.9891	2.3753
a_{10}	1.5630	1.1428	1.2597	1.1796
a_{20}	−0.5630	−0.4291	−0.4661	−0.4725
a_{01}	1.5630	1.1428	1.2597	1.1796
a_{11}	0.8680	1.1454	1.0698	0.5858
a_{21}	−0.3073	−0.4218	−0.3941	−0.2346
a_{02}	−0.5630	−0.4291	−0.4661	−0.4725
a_{12}	−0.3073	−0.4218	−0.3941	−0.2346
a_{22}	0.1135	0.1488	0.1422	0.0940

We also give two examples which have rational coefficients:

$$\begin{aligned} m(x,y) &= \frac{(1+x)(1+y)}{100}(11+6x-2x^2+6y+13xy-4x^2y-2y^2-4xy^2+x^2y^2), \\ m(x,y) &= \frac{(1+x)(1+y)}{3468}(544+120x-52x^2+120y+416xy-128x^2y-52y^2 \\ &\quad -128xy^2+27x^2y^2). \quad \blacksquare \end{aligned}$$

Example 2.4. Let $(\theta,\xi) \in [\pi/4, 7\pi/12] \times [\pi/4, 7\pi/12]$ be fixed. Let

$$\alpha = 3\pi/4 - \arcsin(\sqrt{\sin(\theta+\pi/4)\sin(\xi+\pi/4)}).$$

Set $\eta = \xi$ and $\beta = \alpha$. Then (12) is satisfied. Any θ, ξ give a filter $m(x,y)$ by (10).

Example 2.5. We look for $m(x,y)$ which is in the following form:

$$m(x,y) = \left(\frac{1+x}{2}\right)^2 \left(\frac{1+y}{2}\right)^2 p(x,y)$$

with

$$p(x,y) = a + bx + cy + dxy = (1,x) \begin{bmatrix} a & c \\ b & d \end{bmatrix} \begin{bmatrix} 1 \\ y \end{bmatrix}.$$

The requirement 2° or (2) implies

$$\begin{cases} a^2+b^2+c^2+d^2 = 4, \\ ab+cd = -1, ac+bd = -1, \\ ad = \frac{1}{4}, bc = \frac{1}{4}. \end{cases}$$

From the last two equations, the matrix $\begin{bmatrix} a & c \\ b & d \end{bmatrix}$ is of rank one. Thus, $\begin{bmatrix} a & c \\ b & d \end{bmatrix} = \begin{bmatrix} \alpha \\ \beta \end{bmatrix} [\gamma, \theta]$ and $p(x,y) = [1,x] \begin{bmatrix} \alpha \\ \beta \end{bmatrix} [\gamma,\theta] \begin{bmatrix} 1 \\ y \end{bmatrix}$ which is a tensor product of two polynomials. Hence, $m(x,y)$ is included in Example 2.1. $\blacksquare$

Let ϕ be the scaling function defined in terms of Fourier transform as follows:

$$\hat{\phi}(\omega_1,\omega_2) = \prod_{k=1}^{\infty} m\left(e^{i\frac{\omega_1}{2^k}}, e^{i\frac{\omega_2}{2^k}}\right), \tag{21}$$

where the polynomial $m(x,y)$ is given in (10) and satisfies (12). We now study the orthonormality of the scaling function ϕ. Since m satisfies (2) and (5), we know that $\phi \in L_2(\mathbf{R}^2)$. Let

$$\alpha_{\ell_1,\ell_2} = \int_{\mathbf{R}^2} \phi(x,y)\overline{\phi(x-\ell_1, y-\ell_2)}dxdy, \quad \text{for all} \quad (\ell_1,\ell_2) \in \mathbf{Z}^2. \tag{22}$$

Recalling $m(x,y) = \sum_{0\le k_1,k_2\le 3} c_{k_1,k_2} x^{k_1} y^{k_2}$, we know $\phi(x,y) = 4\sum_{k_1,k_2} c_{k_1,k_2}\phi(2x-k_1, 2y-k_2)$. Using this, (22) implies

$$\alpha_{\ell_1,\ell_2} = 4\sum_{n_1,n_2}\left(\sum_{k_1,k_2} c_{k_1,k_2}c_{k_1+n_1-2\ell_1,k_2+n_2-2\ell_2}\right)\alpha_{n_1,n_2} \tag{23}$$

for any (ℓ_1,ℓ_2), $(n_1,n_2) \in Z^2$. Since support $(\phi) \subset [0,3]^2$, $\alpha_{\ell_1,\ell_2} \neq 0$ for $(\ell_1,\ell_2) \in Z^2 \cap (-3,3)^2$. Let α be a vector of length 25 consisting of $\alpha_{\ell_1\ell_2}$'s for some fixed ordering of indices (ℓ_1,ℓ_2)'s and let A be a matrix of size 25×25 with entries

$$A_{(\ell_1\ell_2),(n_1,n_2)} = 4\sum_{k_1,k_2} c_{k_1k_2}c_{k_1+n_1-2\ell_1,k_2+n_2-2\ell_2}, \tag{24}$$

for the same ordering. Then, $\alpha = A\alpha$. That is, α is an eigenvector of A with eigenvalue 1. Since

$$|m(x,y)|^2 = \sum_{j_1,j_2}\sum_{k_1,k_2} c_{k_1k_2}c_{k_1+j_1,k_2+j_2}x^{j_1}y^{j_2},$$

requirement (2) implies

$$4\sum_{k_1,k_2} c_{k_1k_2}c_{k_1+2j_1,k_2+2j_2} = \delta_{j_1j_2} = \begin{cases} 1, & j_1 = j_2 = 0, \\ 0, & \text{otherwise.} \end{cases}$$

Let δ be a vector of length 25 consisting of δ_{j_1,j_2} for $(j_1,j_2) \in (-3,3)\cap Z^2$. Then $\delta = A\delta$, or δ is also an eigenvector of A with eigenvalue 1. If the eigenvalue 1 is non-degenerate, then $\alpha = \delta$ by the Poisson summation formula, so $\{\phi(x-\ell_1, y-\ell_2), (\ell_1,\ell_2) \in Z^2\}$ is orthonormal. This implies the following.

Theorem 2.2. Let $m(x,y)$ be a polynomial satisfying (2) and $m(1,1) = 1$. Let A be the matrix defined above. Let ϕ be the scaling function generated by $m(e^{i\omega_1}, e^{i\omega_2})$. If 1 is a non-degenerate eigenvalue of A, then $\{\phi(x-\ell_1, y-\ell_2), (\ell_1,\ell_2) \in Z^2\}$ is orthonormal.

This is a generalization of the Lawton condition [10] for orthonormality. We use this condition to check the orthonormality of ϕ generated by filters $m(e^{iw_1}, e^{iw_2})$ given in Examples 2.1–2.4.

Example 2.1. (Continued) Let

$$M(e^{i\omega},\alpha) = h_0 + h_1e^{i\omega} + h_2e^{i2\omega} + h_3e^{i3\omega}$$

with $h_0 = \frac{1}{4} + \frac{1}{2\sqrt{2}}\cos\alpha, h_1 = \frac{1}{4} + \frac{1}{2\sqrt{2}}\sin\alpha, h_2 = \frac{1}{4} - \frac{1}{2\sqrt{2}}\cos\alpha$ and $h_3 = \frac{1}{4} - \frac{1}{2\sqrt{2}}\sin\alpha$. Writing

$$|M(e^{i\omega},\alpha)|^2 = p_0 + p_1(e^{i\omega}+e^{-i\omega}) + p_2(e^{2i\omega}+e^{-2i\omega}) + p_3(e^{i3\omega}+e^{-i3\omega}),$$

we have Lawton's matrix

$$L = 2\begin{bmatrix} p_2 & p_3 & 0 & 0 & 0 \\ p_0 & p_1 & p_2 & p_3 & 0 \\ p_2 & p_1 & p_0 & p_1 & p_2 \\ 0 & p_3 & p_2 & p_1 & p_0 \\ 0 & 0 & 0 & p_3 & p_2 \end{bmatrix} = 2\begin{bmatrix} 0 & p_3 & 0 & 0 & 0 \\ \frac{1}{2} & p_1 & 0 & p_3 & 0 \\ 0 & p_1 & \frac{1}{2} & p_1 & 0 \\ 0 & p_3 & 0 & p_1 & \frac{1}{2} \\ 0 & 0 & 0 & p_3 & 0 \end{bmatrix}$$

since $p_0 = \frac{1}{2}$ and $p_2 = 0$. If 1 is a degenerate eigenvalue of L, then

$$0 = \det\begin{bmatrix} -1 & 2p_3 & 0 & 0 \\ 1 & 2p_1 - 1 & 2p_3 & 0 \\ 0 & 2p_3 & 2p_1 - 1 & 1 \\ 0 & 0 & 2p_3 & -1 \end{bmatrix} = \det\begin{bmatrix} -\frac{1}{2} & 2p_3 \\ 2p_3 & -\frac{1}{2} \end{bmatrix},$$

since $p_1 + p_3 = \frac{1}{4}$. It follows that $p_3 = \pm\frac{1}{4}$. Since $p_3 = h_0 h_3 = \left(\frac{1}{4} + \frac{1}{2\sqrt{2}}\cos\alpha\right)\left(\frac{1}{4} - \frac{1}{2\sqrt{2}}\sin\alpha\right)$, we find that $\alpha = -\frac{\pi}{4}$. In this case, $M(e^{i\omega}, -\pi/4) = \frac{1+e^{i3\omega}}{2}$ which does not generate an orthonormal scaling function. For any other $\alpha \in [0, 2\pi]$, the eigenvalue 1 of L is not degenerate and hence $M(\omega, \alpha)$ will generate an orthonormal scaling function. Hence, $m_0(\omega_1, \omega_2) = M(e^{i\omega_1}, \alpha)M(e^{i\omega_2}, \beta)$ generates an orthonormal scaling function ϕ in $L_2(\mathbf{R}^2)$ if $\alpha \neq -\frac{\pi}{4}$ and $\beta \neq -\frac{\pi}{4}$. ■

Example 2.2.(Continued) Using Theorem 2.2 to check the 8 filters given in Example 2.2, we find that the first 4 filters generate an orthonormal scaling function while the last 4 filters do not. ■

Example 2.3.(Continued) The six filters given in Example 2.3 all generate an orthonormal scaling functions as do the filter based on $(\xi, \eta) \in [\pi/10, 9\pi/10] \times [\pi/3, 19\pi/36]$. ■

Example 2.4.(Continued) This family of filters generate orthonormal scaling functions for $(\theta, \eta) \in [\pi/4, 7\pi/12]^2$.

Next we consider the regularity of the scaling function ϕ generated by filters $m(e^{i\omega_1}, e^{i\omega_2})$ given in Theorem 2.1. To check if $\phi \in C^\gamma(\mathbf{R}^2)$, we study the finiteness of $\int_{\mathbf{R}^2} |\hat{\phi}(\omega)|(1 + |\omega|^\gamma)d\omega$. Write

$$m(e^{i\omega_1}, e^{i\omega_2}) = \frac{1 + e^{i\omega_1}}{2}\frac{1 + e^{i\omega_1}}{2}p(\omega_1, \omega_2).$$

We define an operator P acting on a trigonometric polynomial space $E := \{\sum_{-1 \le j,k \le 1} c_{jk} e^{i(j\omega_1 + k\omega_2)} : c_{j,k} \in \mathbf{R}\}$ by

$$(Pf)(\omega) = \sum_{i=0}^{3} |p\left(\frac{\omega}{2} + \pi_i\right)|^2 f\left(\frac{\omega}{2} + \pi_i\right), \quad \forall f \in E. \tag{25}$$

Theorem 2.3. Let $f_0 = 1$ and λ be the spectral radius of the operator P so that

$$\int_{[-\pi,\pi]^2} (P^n f_0)(\omega)d\omega \le C(\lambda + \delta)^n \tag{26}$$

for a sufficiently small δ. If $\lambda < 2$, then ϕ generated by $m(e^{i\omega_1}, e^{i\omega_2})$ is continuous. Further, $\phi \in C^\gamma(\mathbf{R}^2)$ for $\gamma < (1/2)\log_2(2/\lambda)$.

Proof: It can be checked by induction that

$$\int_{[-\pi,\pi]^2}(P^n f)(\omega)d\omega = \int_{[-2^n\pi,2^n\pi]^2} f\left(\frac{\omega}{2^n}\right)\prod_{k=1}^{n}|p\left(\frac{\omega}{2^k}\right)|^2 d\omega.$$

Then for $\gamma < \varepsilon < \frac{1}{2}$,

$$\begin{aligned}
&\int_{\mathbf{R}^2}|\hat{\phi}(\omega)|(1+|\omega|^\gamma)d\omega = \int_{\mathbf{R}^2}\left|\frac{\sin\frac{\omega_1}{2}}{\frac{\omega_1}{2}}\frac{\sin\frac{\omega_2}{2}}{\frac{\omega_2}{2}}\right|(1+|\omega|^\gamma)\prod_{k=1}^{\infty}|p\left(\frac{\omega}{2^k}\right)|d\omega \\
\leq\ & \left(\int_{\mathbf{R}^2}\left|\frac{\sin\frac{\omega_1}{2}}{\frac{\omega_1}{2}}\frac{\sin\frac{\omega_2}{2}}{\frac{\omega_2}{2}}\right|^{1+2\varepsilon}(1+|\omega|)^{2\gamma}d\omega\right)^{\frac{1}{2}}\left(\int_{\mathbf{R}^2}\left|\frac{\sin\frac{\omega_1}{2}}{\frac{\omega_1}{2}}\frac{\sin\frac{\omega_2}{2}}{\frac{\omega_2}{2}}\right|^{1-2\varepsilon}\prod_{k=1}^{\infty}|p\left(\frac{\omega}{2^k}\right)|^2 d\omega\right)^{\frac{1}{2}} \\
\leq\ & O\left(\frac{1}{(\varepsilon-\gamma)}\right)\left(1+\sum_{n=1}^{\infty}\int_{\substack{2^{n-1}\pi\leq|\omega_1|\leq 2^n\pi \\ 2^{n-1}\pi\leq|\omega_2|\leq 2^n\pi}} 2^{-n(1-2\varepsilon)}\prod_{k=1}^{n}|p\left(\frac{\omega}{2^k}\right)|^2 d\omega\right)^{\frac{1}{2}} \\
=\ & O\left(\frac{1}{\varepsilon-\gamma}\right)\left(1+c_1\sum_{n=1}^{\infty}2^{-n(1-2\varepsilon)}\int_{[-\pi,\pi]^2}(P^n f_0)(\omega)d\omega\right)^{\frac{1}{2}} \\
\leq\ & O\left(\frac{1}{\varepsilon-\gamma}\right)\left(1+\sum_{n=1}^{\infty}2^{-n(1-2\varepsilon)}C(\lambda+\delta)^n\right)^{\frac{1}{2}}
\end{aligned}$$

for δ sufficiently small. Hence, $\phi \in C^\gamma(\mathbf{R}^2)$ if $2^{-n(1-2\varepsilon)}\lambda^n < 1$. This implies $\lambda < 2$. ∎

We now apply Theorem 2.3 to check the regularity of the scaling functions generated by the filters given in Examples 2.1–2.4.

Example 2.1. (Continued) Recalling $M(x,\alpha)$ from (19), let

$$p(\omega) = \frac{1}{2} + \frac{\sqrt{2}}{2}\cos\alpha + \frac{\sqrt{2}}{2}(\sin\alpha - \cos\alpha)e^{i\omega} + \left(\frac{1}{2} - \frac{\sin\alpha}{\sqrt{2}}\right)e^{i2\omega}.$$

Then $|p(\omega)|^2 = q_0 + q_1(e^{i\omega}+e^{-i\omega}) + q_2(e^{i2\omega}+e^{-i2\omega})$ with

$$\begin{aligned}
q_0 &= \frac{3}{2} + \frac{1}{\sqrt{2}}(\cos\alpha - \sin\alpha) - \sin\alpha\cos\alpha, \\
q_1 &= -\frac{1}{2} - \frac{1}{\sqrt{2}}(\cos\alpha - \sin\alpha) + \sin\alpha\cos\alpha = 1 - q_0, \\
q_2 &= \frac{1}{4} + \frac{1}{2\sqrt{2}}(\cos\alpha - \sin\alpha) - \frac{1}{2}\sin\alpha\cos\alpha = \frac{1}{2}(q_0 - 1).
\end{aligned}$$

Define by

$$Pf(2\omega) = |p(\omega)|^2 f(\omega) + |p(\omega+\pi)|^2 f(\omega+\pi).$$

If $f_0(\omega) = 1$, then $Pf_0(2\omega) = 2q_0 + 2q_2(e^{i\omega}+e^{-i\omega})$. If $f_1(\omega) = e^{i\omega}+e^{-i\omega}$, then $Pf_1(2\omega) = 4q_1 + 2q_1(e^{i\omega}+e^{-i\omega})$. Thus, under the basis $\{f_0, f_1\}$, the matrix form of P is $P = \begin{bmatrix} 2q_0 & 2q_2 \\ 4q_1 & 2q_1 \end{bmatrix}$. The eigenvalues of P are

$$\lambda = 1 \pm \sqrt{4q_0 - 3} = \begin{cases} 1 \pm \sqrt{4q_0-3}, & \text{if } 4q_0 \geq 3 \\ 2\sqrt{1-q_0}, & \text{if } 4q_0 < 3. \end{cases}$$

By Theorem 2.3, in order to have $\phi \in C(\mathbf{R})$ generated by the filter $M(e^{i\omega}, \alpha)$, we need to have $\lambda < 2$. It follows that $0 < q_0 < 1$. This requires

$$-\sqrt{2} < \cos\alpha - \sin\alpha < 0.$$

Thus, if $\alpha \neq -\pi/4$ and $\beta \neq -\pi/4$ satisfy

$$-\sqrt{2} < \cos\alpha - \sin\alpha < 0 \text{ and } -\sqrt{2} < \cos\beta - \sin\beta < 0,$$

then $M(e^{i\omega_1}, \alpha)M(e^{i\omega_1}, \beta)$ generates a continuous orthonormal scaling function ϕ supported on $[0,3] \times [0,3]$. For other α, we refer to [14] where Colella and Heil gave a detail study of the continuity of the orthonormal scaling functions supported on $[0,3]$ in the univariate setting. ■

Example 2.2. (Continued) All ϕ generated by m given in Example 2.2 are only in $L_2(\mathbf{R}^2)$, none are continuous. ■

Example 2.3. (Continued) Let

$$\begin{aligned} p(\omega_1, \omega_2) &= a_0 0 + a_{10}e^{i\omega_1} + a_{01}e^{i\omega_2} + a_{11}e^{i(\omega_1+\omega_2)} + a_{20}e^{i2\omega_1} + a_{21}e^{i(2\omega_1+\omega_2)} \\ &\quad + a_{22}e^{i2(\omega_1+\omega_2)} + a_{12}e^{i(\omega_1+2\omega_2)} + a_{02}e^{i2\omega_2}. \end{aligned}$$

for a_{jk}'s given in (10). Define

$$\begin{aligned} Pf(2\omega_1, 2\omega_2) &= |p(\omega_1, \omega_2)|^2 f(\omega_1, \omega_2) + |p(\omega_1 + \pi, \omega_2)|^2 f(\omega_1 + \pi, \omega_2) \\ &\quad + |p(\omega_1, \omega_2 + \pi)|^2 f(\omega_1, \omega_2 + \pi) + |p(\omega_1 + \pi, \omega_2 + \pi)|^2 f(\omega_1 + \pi, \omega_2 + \pi). \end{aligned}$$

If $f_0(\omega_1, \omega_2) = 1$, then

$$Pf_0(2\omega_1, 2\omega_2) = \sum_{\nu=0}^{4} q_{0,\nu} f_\nu(2\omega_1, 2\omega_2)$$

with

$$\begin{aligned} f_1(\omega_1, \omega_2) &= e^{i\omega_1} + e^{-i\omega_1}, f_3(\omega_1, \omega_2) = e^{i(\omega_1+\omega_2)} + e^{-i(\omega_1+\omega_2)}, \\ f_2(\omega_1, \omega_2) &= e^{i\omega_2} + e^{-i\omega_2}, f_4(\omega_1, \omega_2) = e^{i(\omega_1-\omega_2)} + e^{-i(\omega_1-\omega_2)}. \end{aligned}$$

Then $Pf_\nu(2\omega_1, 2\omega_2) = \sum_{\mu=0}^{4} q_{\nu,\mu} f_\mu(2\omega_1, 2\omega_2)$. Under the basis $\{f_0, f_1, f_2, f_3, f_4\}$, the matrix for the P is $[q_{\mu,\nu}]_{0 \le \mu,\nu \le 4}$. The spectral radius for the four explicit solution sets listed in Example 2.3 is less than 2, while the spectral radius for the filters with rational coefficients is not less than 2. By Theorem 2.3, the corresponding filters Ex.2.3.1–2.3.4 generate continuous orthonormal scaling functions supported on $[0,3] \times [0,3]$. We plot the largest eigenvalue as a function of $(\xi, \eta) \in [\pi/10, 9\pi/10] \times [\pi/3, 19\pi/36]$ in Fig. 1. ■

Example 2.4. (Continued) Theorem 2.3 implies all scaling functions from Example 2.4 within the contour line $\lambda = 2$ as shown in Fig. 2 have certain Hölder continuity. ■

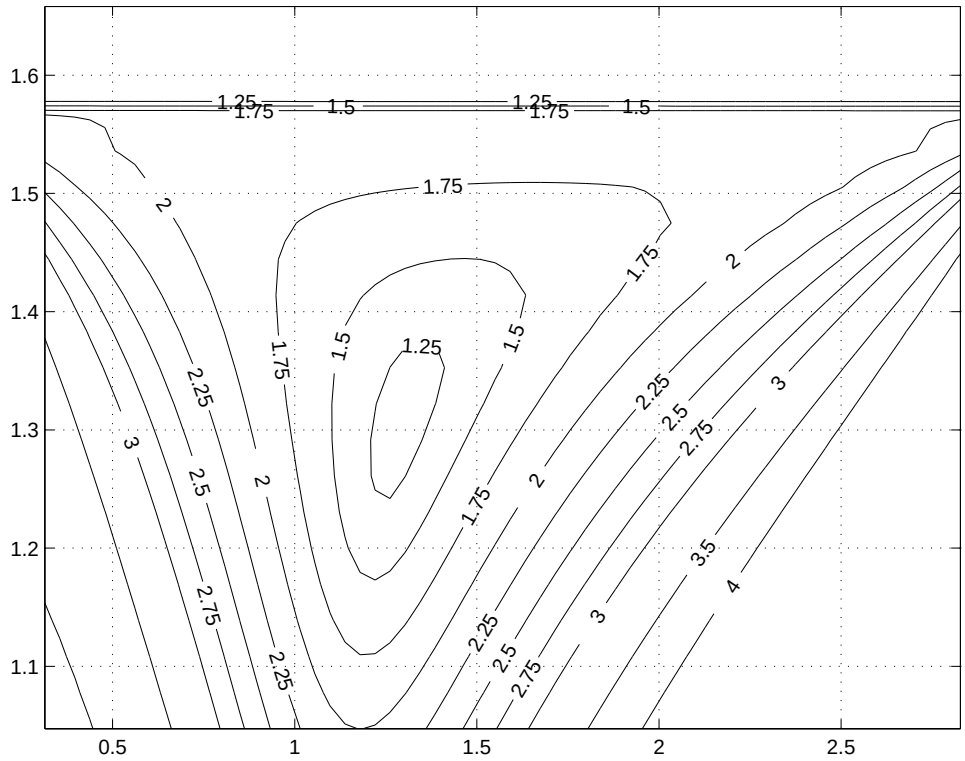

Figure 1. Contour of spectrum λ based on $(\xi, \eta) \in [\pi/10, 9\pi/10] \times [\pi/3, 19\pi/36]$

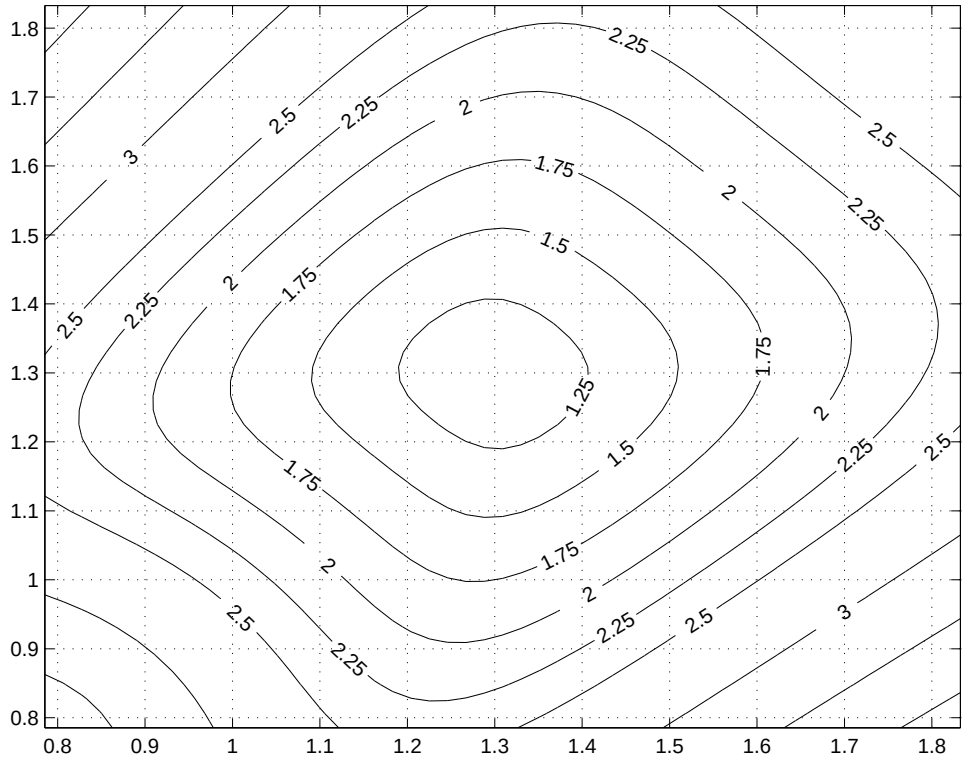

Figure 2. Contour of spectrum λ based on $(\theta, \xi) \in [\pi/4, 7\pi/12]^2$

Finally, we show how to construct wavelets associated with the scaling ϕ generated by m given in Theorem 2.1 which satisfies the conditions in Theorem 2.2.

First, for the linear phase filters given in Example 2.2, we can find m_ν satisfying requirement 5° as follows: Since $\overline{m(\omega_1,\omega_2)} = e^{-3i(\omega_1+\omega_2)}m(\omega_1,\omega_2)$, the following matrix is unitary

$$\begin{bmatrix} m(\omega_1,\omega_2) & m(\omega_1+\pi,\omega_2) & m(\omega_1,\omega_2+\pi) & m(\omega_1+\pi,\omega_2+\pi) \\ m_1(\omega_1,\omega_2) & m_1(\omega_1+\pi,\omega_2) & m_1(\omega_1,\omega_2+\pi) & m_1(\omega_1+\pi,\omega_2+\pi) \\ m_2(\omega_1,\omega_2) & m_2(\omega_1+\pi,\omega_2) & m_2(\omega_1,\omega_2+\pi) & m_2(\omega_1+\pi,\omega_2+\pi) \\ m_3(\omega_1,\omega_2) & m_3(\omega_1+\pi,\omega_2) & m_3(\omega_1,\omega_2+\pi) & m_3(\omega_1+\pi,\omega_2+\pi) \end{bmatrix}$$

where

$$\begin{cases} m_1(\omega_1,\omega_2) = e^{i\omega_1}\overline{m(\omega_1+\pi,\omega_2)} \\ m_2(\omega_1,\omega_2) = e^{i(\omega_1+\omega_2)}\overline{m(\omega_1,\omega_2+\pi)} \\ m_3(\omega_1,\omega_2) = e^{i\omega_1}\overline{m(\omega_1+\pi,\omega_2+\pi)}. \end{cases} \tag{27}$$

For other filters, we construct m_ν by a different method. We begin with polyphase components f_0, f_1, f_2, f_3 of $m(x,y)$. Write $[f_0,f_1,f_2,f_3]^T = \mathbf{a} + x\mathbf{b} + y\mathbf{c} + xy\mathbf{d}$ with $\mathbf{a} = (a_1,a_1,a_2,a_3)^T$ and etc.. Let $L = [\mathbf{a},\mathbf{b},\mathbf{c},\mathbf{d}]$ be a 4×4 matrix. Then there exists an orthonormal matrix H (by the Householder transform) such that HL is a lower triangular matrix. Then

$$\begin{bmatrix} \tilde{f}_0 \\ \tilde{f}_1 \\ \tilde{f}_2 \\ \tilde{f}_3 \end{bmatrix} = H \begin{bmatrix} f_0 \\ f_1 \\ f_2 \\ f_3 \end{bmatrix} = HL \begin{bmatrix} 1 \\ x \\ y \\ xy \end{bmatrix} = \begin{bmatrix} \times & 0 & 0 & 0 \\ \times & \times & 0 & 0 \\ \times & \times & \times & 0 \\ \times & \times & \times & \times \end{bmatrix} \begin{bmatrix} 1 \\ x \\ y \\ xy \end{bmatrix}.$$

Note that, by (3),

$$|\tilde{f}_0|^2 + |\tilde{f}_1|^2 + |\tilde{f}_2|^2 + |\tilde{f}_3|^2 = |f_0|^2 + |f_1|^2 + |f_2|^2 + |f_3|^2 = \frac{1}{4}.$$

If $|\tilde{f}_0| = \frac{1}{2}$, then $\tilde{f}_1 = \tilde{f}_2 = \tilde{f}_3 = 0$ and we are done. Otherwise, let

$$v = [\tilde{f}_0,\tilde{f}_1,\tilde{f}_2,\tilde{f}_3]^T - \frac{1}{2}[1,0,0,0]^T \text{ and } H(v) = I_4 - \frac{2}{v^*v}vv^*$$

be a Householder matrix such that

$$H(v)\begin{bmatrix} \tilde{f}_0 \\ \tilde{f}_1 \\ \tilde{f}_2 \\ \tilde{f}_3 \end{bmatrix} = \begin{bmatrix} 1/2 \\ 0 \\ 0 \\ 0 \end{bmatrix}.$$

For convenience, let $H(v)$ be either an identity matrix of size 4×4 if $|\tilde{f}_0| = \frac{1}{2}$ or the Householder matrix $H(v)$ above. Then we have

$$\begin{bmatrix} f_0 \\ f_1 \\ f_2 \\ f_3 \end{bmatrix} = HH(v)\begin{bmatrix} 1/2 \\ 0 \\ 0 \\ 0 \end{bmatrix}.$$

It follows that

$$[f_0, f_1, f_2, f_3] = \left[\frac{1}{2}, 0, 0, 0\right] H(v)H.$$

By choosing $M(x,y) = \frac{1}{2}H(v)H$, we have

$$M(x,y)M^*(x,y) = \frac{1}{4}I_4$$

with $[f_0, f_1, f_2, f_3]$ in the first row of $M(x,y)$. We should note that all entries of $M(x,y)$ are polynomials of x and y since v^*v is a constant and H is a constant matrix. We now define polynomials m_ν, $\nu = 0,1,2,3$ with $m_0(\omega) = m(e^{i\omega_1}, e^{i\omega_2})$ as follows:

$$\begin{bmatrix} m_0(\omega+\pi_0) & m_0(\omega+\pi_1) & m_0(\omega+\pi_2) & m_0(\omega+\pi_3) \\ m_1(\omega+\pi_0) & m_1(\omega+\pi_1) & m_1(\omega+\pi_2) & m_1(\omega+\pi_3) \\ m_2(\omega+\pi_0) & m_2(\omega+\pi_1) & m_2(\omega+\pi_2) & m_2(\omega+\pi_3) \\ m_3(\omega+\pi_0) & m_3(\omega+\pi_1) & m_3(\omega+\pi_2) & m_3(\omega+\pi_3) \end{bmatrix}$$

$$= M(e^{2i\omega_1}, e^{2i\omega_2}) \begin{bmatrix} 1 & 1 & 1 & 1 \\ 1 & -1 & 1 & -1 \\ 1 & 1 & -1 & -1 \\ 1 & -1 & -1 & 1 \end{bmatrix} \begin{bmatrix} 1 & 0 & 0 & 0 \\ 0 & e^{i\omega_1} & 0 & 0 \\ 0 & 0 & e^{i\omega_2} & 0 \\ 0 & 0 & 0 & e^{i\omega_1+\omega_2} \end{bmatrix}. \tag{28}$$

Theorem 2.4. Let m_ν be trigonometric polynomials constructed in (28) above. Let ϕ be the scaling function generated by m_0 by (21), where m_0 is given in Theorem 2.1 and satisfies the conditions in Theorem 2.2. Let ψ_ν be the wavelets defined by

$$\hat{\psi}_\nu(\omega) = m_\nu(\omega/2)\,\hat{\phi}(\omega/2), \nu = 1,2,3. \tag{29}$$

Then

$$\left\{2^k \psi_\nu\left(2^k x - \ell_1, 2^k - \ell_2\right) : \quad (\ell_1, \ell_2) \in \mathbf{Z}^2, k \in Z, \nu = 1,2,3\right\}$$

is an orthonormal basis for $L_2(\mathbf{R})$.

The proof is standard based on multi-resolution analysis of $L_2(\mathbf{R}^2)$ (cf. [11] for the univariate setting).

3. NUMERICAL EXPERIMENTS AND REMARKS

Let f be an image with finite energy, i.e., $f \in L_2(\mathbf{R}^2)$. Let $s_{j,k} = f(j/2^\ell, k/2^\ell), (j,k) \in \mathbf{Z}^2$ be the digitization of f, where $1/2^\ell$ is a sampling step. To use the wavelets constructed in this paper for image processing, we first approximate f by

$$A_\ell(f) := \sum_{(j,k)\in \mathbf{z}^2} s_{jk}^{(\ell)} \phi(2^\ell x - j, 2^\ell y - k)$$

where ϕ is an orthonormal continuous scaling function constructed in the previous section. Since $\hat{\phi}(2j\pi, 2k\pi) = 0$ for all $(j,k) \in \mathbf{Z}^2 \backslash \{(0,0)\}$, we have

$$1 = \sum_{(j,k)\in \mathbf{z}^2} \phi(x-j, y-k), \qquad \text{for each } (x,y) \in \mathbf{R}^2.$$

Since ϕ has compact support, it follows that $A_\ell(f)$ converges to f pointwise as $\ell \longrightarrow \infty$ if f is a continuous function.

Let $V_0 = \text{span}_{L_2}\{\phi(x-j, y-k) : (j,k) \in \mathbf{Z}^2\}$ and $V_k := \{g(2^k \cdot), \forall g \in V_0\}$ for all $k \in \mathbf{Z}$. Writing $\psi_\nu, \nu = 1, 2, 3$ for the wavelets associated with ϕ constructed by the method discussed in the previous section, let $W_{0,\nu} := \text{span}_{L_2}\{\psi_\nu(x-j, y-k) : (j,k) \in \mathbf{Z}^2\}$ and $W_{k,\nu} := \{g(2^k \cdot) : \forall g \in W_{0,\nu}\}$. Then $V_k \subset V_{k+1}$ for all $k \in \mathbf{Z}$ by (21). It can be shown that $\{V_k, k \in \mathbf{Z}\}$ forms a multi-resolution analysis of $L_2(\mathbf{R}^2)$. By 5°, we know that $V_1 = V_0 \oplus W_{0,1} \oplus W_{0,2} \oplus W_{0,3}$. Without loss of generality, we may assume that $\ell = 1$. It is clear that $A_1(f) \in V_1$. By the relation above, we may express the approximate image $A_1(f)$ by sub-images in $V_0, W_{0,1}, W_{0,2}$, and $W_{0,3}$.

Recall (21) and (29) in the previous section. It follows from 5° that

$$\hat{\phi}(\omega/2) = \sum_{\nu=0}^{3} \sum_{k=0}^{3} \overline{m_\nu(\omega/2 + \pi_k)} \hat{\psi}_\nu(\omega)$$

with $\psi_0 := \phi$. In the frequency domain, writing $F(\omega) = \sum_{(j,k)\in\mathbf{Z}^2} f_{jk} e^{-i(j\omega_1 + k\omega_2)}$, we have

$$\begin{aligned} \widehat{A_1(f)}(\omega) &= F(\omega/2)\hat{\phi}(\omega/2) \\ &= \sum_{\nu=0}^{3} \sum_{k=0}^{3} \overline{m_\nu(\omega/2 + \pi_k)} F(\omega/2) \hat{\psi}_\nu(\omega). \end{aligned}$$

Let us denote the four terms in the above summation by

$$\begin{aligned} \widehat{A_0(f)}(\omega) &:= \sum_{k=0}^{3} \overline{m_0(\omega/2 + \pi_k)} F(\omega/2)\hat{\phi}(\omega) \\ \widehat{D_{0,\nu}(f)}(\omega) &:= \sum_{k=0}^{3} \overline{m_\nu(\omega/2 + \pi_k)} F(\omega/2)\hat{\psi}_\nu(\omega), \qquad \nu = 1, 2, 3. \end{aligned}$$

In the time domain, we write

$$\begin{aligned} A_0(f) &= \sum_{(j,k)\in\mathbf{Z}^2} f_{0,j,k}\phi(x-j, y-k) \in V_0 \\ D_{0,\nu}(f) &= \sum_{(j,k)\in\mathbf{Z}^2} g_{0,\nu,j,k}\psi_\nu(x-j, y-k) \in W_{0,\nu}, \nu = 1, 2, 3. \end{aligned}$$

The computation of $\{f_{0,j,k} : (j,k) \in \mathbf{Z}^2\}$ is equivalent to the convolution of $\{c_{j,k} : 0 \le j, k \le 3\}$ with $\{f_{j,k} : (j,k) \in \mathbf{Z}^2\}$ and down-sampling by 2, where $c_{j,k}$'s are given in (10). Similarly, for the digital sub-images $\{g_{0,\nu,j,k} : (j,k) \in \mathbf{Z}^2\}$. Such a decomposition of $A_1(f)$ into $A_0(f)$ and $D_{0,\nu}(f)$ may be carried out repeatedly.

On the other hand, when we have $A_0(f)$ and $D_{0,\nu}(f)$, we can reconstruct $A_1(f)$ exactly. Indeed, recalling (21) and (29), we have,

$$\begin{aligned} \widehat{A_0(f)}(\omega) &= F_0(\omega)m_0(\omega/2)\hat{\phi}(\omega/2), \\ \widehat{D_{0,\nu}(f)}(\omega) &= G_{0,\nu}(\omega)m_\nu(\omega/2)\hat{\phi}(\omega/2), \nu = 1, 2, 3, \end{aligned}$$

where F_0 and $G_{0,\nu}$ denote the discrete Fourier transform of the digital sub-images $\{f_{0,j,k}, (j,k) \in \mathbf{Z}^2\}$ and $\{g_{0,\nu,j,k} : (j,k) \in \mathbf{Z}^2\}$. By adding the four terms above together, we recover $\widehat{A_1(f)}(\omega)$. In the time domain, the computation of $F_0(\omega)m_0(\omega/2)$ is equivalent to up-sampling the sub-image $\{f_{0,j,k} : (j,k) \in \mathbf{Z}^2\}$ by 2 and then convoluting with $\{c_{j,k} : 0 \le j,k \le 3\}$. Similarly, for the computation of $G_{0,\nu}(\omega)m_\nu(\omega/2)$. The reconstruction is exact because that the filters $m_\nu, \nu = 0,1,2,3$, satisfy 2°.

Let us first present an interesting example of those four filters m_ν's below, although the scaling function and wavelets associated with these filters are not continuous.

Table 1. The coefficients of trigonometric polynomial $m_\nu(e^{i\omega_1}, e^{i\omega_2})$ with the constant term in the lower and left corner, $\nu = 0,1,2,3$.

$m_0 =$

0.12438	0.124065	0.134125	0.134441
0.125309	−0.124997	−0.116181	0.134125
0.116492	−0.13257	−0.124997	0.124065
0.115563	0.116492	0.125309	0.12438

$m_1 =$

0.119815	0.103642	−0.128752	−0.129055
0.136266	−0.120253	0.111526	−0.128752
0.117017	−0.143438	0.124518	−0.114555
0.132964	0.142446	−0.124211	−0.114869
0.00393323	−0.0044761	−0.00422041	0.00418892
0.00390188	0.00393323	0.00423092	0.00419957

$m_2 =$

0	0	0.000127888	0.000110625	−0.000137428	−0.000137751
0	0	0.000145448	−0.000128356	0.000119041	−0.000137428
0.129237	0.111792	0.130945	0.115243	−0.00406622	−0.00433127
0.146981	−0.129709	−0.106902	0.107394	0.00350473	−0.00432173
−0.120619	0.137267	0.125783	−0.124314	0.00390884	−0.00387968
−0.119657	−0.120619	−0.133362	−0.132429	−0.00391858	−0.00388954

$m_3 =$

0.124063	0.107316	−0.137383	−0.137147	0.00436924	0.00437951
0.141097	−0.124516	0.110856	−0.129236	−0.00378467	0.00436924
−0.111723	0.135288	−0.12695	0.116734	−0.00407191	0.00404148
−0.110242	−0.11987	0.134239	0.125177	0.00408205	0.00405175
−0.0037948	0.00431857	0.00407185	−0.00404147	0	0
−0.00376455	−0.0037948	−0.00408203	−0.00405178	0	0

We have experimented with the decomposition and reconstruction procedures using several well-known images. In Fig. 3 we show the decompositions of Lenna and a fingerprint. We may compare them with the decomposition by separable filters, e.g., the filter associated with Daubechies' scaling function and wavelet ${}_2\phi$ and ${}_2\psi$. We can see that the sub-images in the high frequency bands in Fig. 3 reveal more features than does the separable filter in Fig. 4.

These four filters may find an application in the analysis of images of an electronic circuit. Since many different gateways look similar in the horizontal and vertical sub-images when an image of

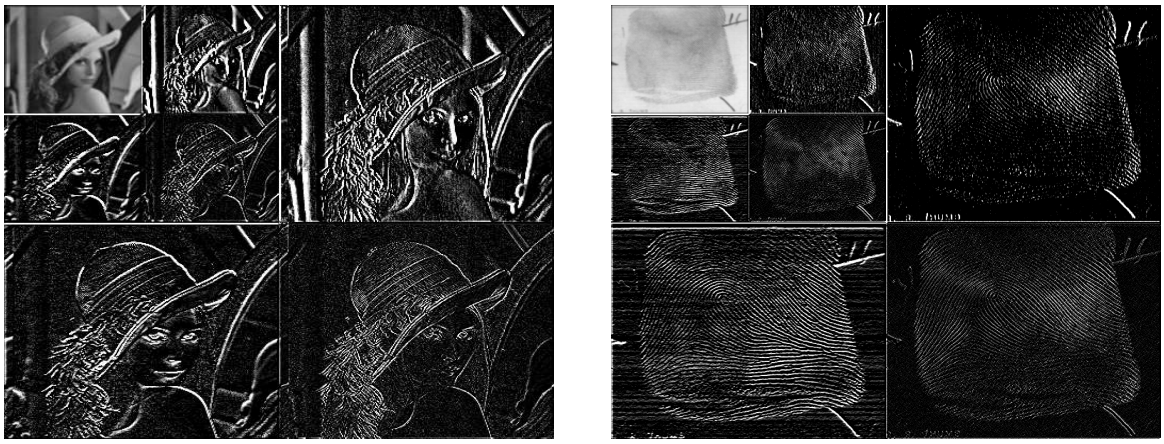

Figure 3. Decomposition by a non-separable filter given in Table 1.

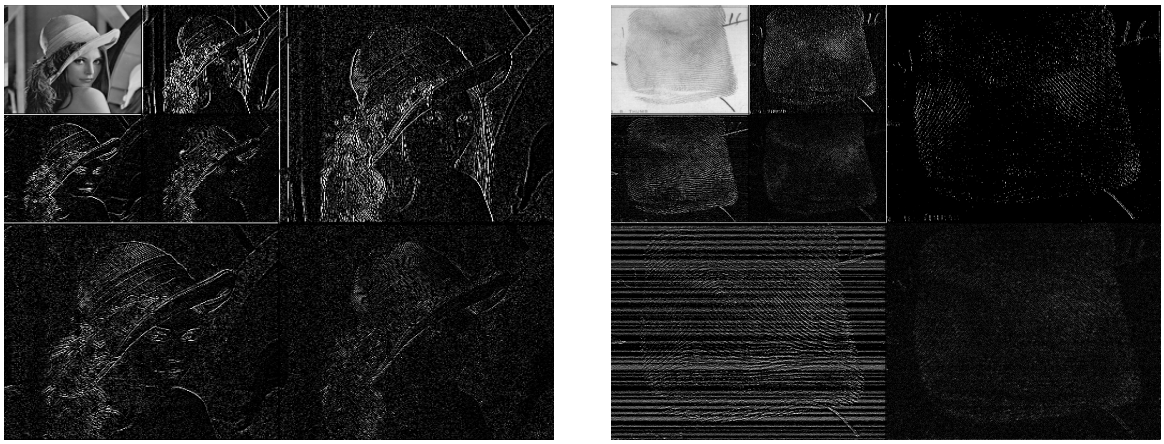

Figure 4. Decomposition by a separable filter associated with Daubechies' scaling function ${}_2\phi$

a circuit is decomposed into low-pass and three high-pass band sub-images, the diagonal bandpass sub-image may be a key to differentiate the gateway types.

We have also implemented an image compression scheme using the non-separable wavelets and compared with the tensor product Haar, Daubechies wavelets D4 and D6, and the well-known biorthogonal wavelets with lengths 9 and 7 which are the wavelets for FBI finger print compression standard. The image compression scheme consists of multilevel wavelet decomposition, embedded zero-tree encoding and decoding [12], multilevel wavelet reconstruction, peak signal to noise ratio(PSNR) error analysis.

The embedded zero-tree encoding and decoding algorithm consists of scalar quantization with a coded significance map which maps spatial relevance across scales. That is, small coefficients in the coarser scales will correspond to small coefficients in all the finer scales at the same spatial location. The embedded aspect is a binary code which intertwines the significance map with the thresholding values. The coding process yields an actual compressed file whose size is compared to the original binary gray-scale image file which contains a byte per pixel.

This coding scheme is currently respected as one of the best wavelet encoders available for image compression. For this experiment, periodic boundaries were employed for both the separable and non-separable wavelets.

The peak signal to noise ratio(PSNR) for a gray-scale image x and its compressed reconstruction $\hat{x}$ is given by

$$\begin{aligned} RMSE &= \sqrt{\frac{\sum_{i\le M, j\le N} (x_{i,j} - \hat{x}_{i,j})^2}{NM}}, \\ PSNR &= 20 \log_{10} \left(\frac{255}{RMSE} \right). \end{aligned}$$

Because this application is image dependent, we have chosen three images: a text image shown on the left of Figure 5 besides the standard Lenna image and a finger-print image of size 512×512 in Figure 3.

Table 2. PSNR Image Compression Comparison

Compression Ratio 5:1			
Images	Text	Lenna	Finger
Tensor Haar	44.2946	39.5135	35.0276
Tensor D4	35.9717	40.3629	36.8700
Tensor D6	35.4661	40.6019	37.3612
Tensor 9/7	35.4661	41.1259	37.7037
Non-separable	44.3010	40.2244	36.8700

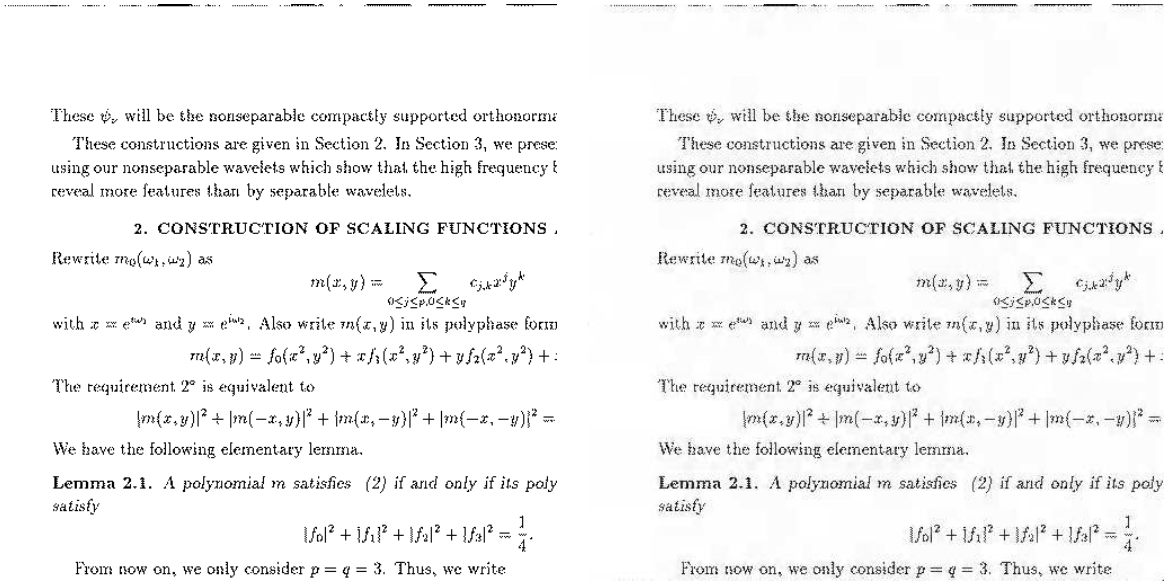

These ψ_ν will be the nonseparable compactly supported orthonorma

These constructions are given in Section 2. In Section 3, we prese using our nonseparable wavelets which show that the high frequency reveal more features than by separable wavelets.

2. CONSTRUCTION OF SCALING FUNCTIONS

Rewrite $m_0(\omega_1, \omega_2)$ as

$$m(x,y) = \sum_{0\le j\le p, 0\le k\le q} c_{j,k} x^j y^k$$

with $x = e^{i\omega_1}$ and $y = e^{i\omega_2}$. Also write $m(x,y)$ in its polyphase form

$$m(x,y) = f_0(x^2,y^2) + xf_1(x^2,y^2) + yf_2(x^2,y^2) +$$

The requirement 2° is equivalent to

$$|m(x,y)|^2 + |m(-x,y)|^2 + |m(x,-y)|^2 + |m(-x,-y)|^2 =$$

We have the following elementary lemma.

Lemma 2.1. *A polynomial m satisfies (2) if and only if its poly satisfy*

$$|f_0|^2 + |f_1|^2 + |f_2|^2 + |f_3|^2 = \frac{1}{4}.$$

From now on, we only consider $p = q = 3$. Thus, we write

These ψ_ν will be the nonseparable compactly supported orthonorma

These constructions are given in Section 2. In Section 3, we prese using our nonseparable wavelets which show that the high frequency reveal more features than by separable wavelets.

2. CONSTRUCTION OF SCALING FUNCTIONS

Rewrite $m_0(\omega_1, \omega_2)$ as

$$m(x,y) = \sum_{0\le j\le p, 0\le k\le q} c_{j,k} x^j y^k$$

with $x = e^{i\omega_1}$ and $y = e^{i\omega_2}$. Also write $m(x,y)$ in its polyphase form

$$m(x,y) = f_0(x^2,y^2) + xf_1(x^2,y^2) + yf_2(x^2,y^2) +$$

The requirement 2° is equivalent to

$$|m(x,y)|^2 + |m(-x,y)|^2 + |m(x,-y)|^2 + |m(-x,-y)|^2 =$$

We have the following elementary lemma.

Lemma 2.1. *A polynomial m satisfies (2) if and only if its poly satisfy*

$$|f_0|^2 + |f_1|^2 + |f_2|^2 + |f_3|^2 = \frac{1}{4}.$$

From now on, we only consider $p = q = 3$. Thus, we write

Figure 5. A Text Image (left) and Reconstructed Image after 10:1 Compression(right)

Compression Ratio 10:1			
Images	Text	Lenna	Finger
Tensor Haar	24.2022	35.3078	31.5978
Tensor D4	25.2776	36.5947	32.5100
Tensor D6	24.8288	36.9106	32.8931
Tensor 9/7	24.7949	38.1000	33.0980
Non-separable	26.5489	36.4201	32.560

Compression Ratio 15:1			
Images	Text	Lenna	Finger
Tensor Haar	20.3240	32.8821	30.1455
Tensor D4	21.3618	35.1661	31.0029
Tensor D6	20.9433	35.5861	31.0523
Tensor 9/7	20.9693	35.8116	32.0364
Non-separable	21.9141	34.9405	30.6138

We can see that our non-separable wavelets do a significantly better job for the text image for compression ratios 10 and 15. This may find an application for fax transmission. We should remark that the non-separable filters in the numerical experiments above are in Example 2.4 and we did not exhaust all the possible non-separable filters in Theorem 2.1.

Finally, we have the following two remarks in order.

Remark 1. It is very easy to implement the filters constructed in this paper. In particular, for

a filter m_ν, we express the coefficient matrix in singular value form, i.e., $[c_{\nu,ij}]_{0\le i,j\le 3} = \sum_{k=1}^{4} \sigma_i \mathbf{v}_k \mathbf{u}_k^T$. with singular values σ_k's and singular vectors $\mathbf{v}_k$'s and $\mathbf{u}_k$'s. Then the processing of the convolution of m_ν with any digital image $\{s_{ij}\}$ is the same as the processing of the convolution of separable filters (cf. [13]) $\mathbf{v}_k$ and $\mathbf{u}_k^T$ with $\{s_{ij}\}$ for $k = 1, 2, 3, 4$ and then addition of the resulting convolutions multiplied by appropriate singular values.

Remark 2. It would be interesting to construct continuous compactly supported scaling functions and wavelets associated with a linear phase filter. The authors are able to obtain a complete solution of the linear phase filters of size 6x6 satisfying $1°, 2°$, and $6°$ (cf. [15]).

ACKNOWLEDGMENTS

The authors would like to thank David Roach for his help in the implementation of the non-separable wavelets for the image compression.

REFERENCES

1. S. D. Riemenschneider and Z. Shen, "Box splines, cardinal series, and wavelets," in *Approximation Theory and Functional Analysis*, C. K. Chui, ed., pp. 133–149, Academic Press, Boston, 1991.
2. C. K. Chui, J. Stockler, and J. D. Ward, "Compactly supported box-spline wavelets," *Approx. Theory Appl.* **8**, pp. 77–100, 1992.
3. A. Cohen and J. M. Schlenker, "Compactly supported bidimensional wavelet bases with hexagonal symmetry," *Constr. Approx.* **9**, pp. 209–236, 1993.
4. S. D. Riemenschneider and Z. Shen, "Wavelets and pre-wavelets in low dimensions," *J. Approx. Theory* **71**, pp. 18–38, 1992.
5. W. He and M. J. Lai, "Construction of bivariate compactly supported biorthogonal box spline wavelets with arbitrarily high regularities," *Applied Comput. Harmonic Analysis* **6**, pp. 53–74, 1999.
6. A. Cohen and I. Daubechies, "Nonseparable dimensional wavelet bases," *Revista Mat. Iberoamericana* **9**, pp. 51–137, 1993.
7. I. Daubechies, "Orthonormal bases of compactly supported wavelets," *Comm. Pure Appl. Math.* **41**, pp. 909–996, 1988.
8. J. Kovačević and M. Vetterli, "Nonseparable multidimensional perfect reconstruction filter banks and wavelet bases for $\mathbf{r}^n$," *IEEE Trans. Info. Theory* **38**, pp. 533–555, 1992.
9. I. Daubechies, *Ten Lectures on Wavelets*, SIAM, Philadelphia, 1992.
10. W. Lawton, "Necessary and sufficient conditions for constructing orthonormal wavelet bases," *J. Math. Phys.* **32**, pp. 57–61, 1991.
11. S. G. Mallat, "Multiresolution approximations and wavelet orthonormal bases of $l^2(r)$," *Trans. Amer. Math. Society* **315**, pp. 69–87, 1989.

12. A. Said and W. A. Pearlman, "A new fast and efficient image codec based on set partitioning in hierarchical trees," *IEEE Transactions on Circuits and Systems for Video Technology* **6**, pp. 243–250, 1996.
13. S. G. Mallat, "A theory of multiresolution signal decomposition: the wavelet representation," *IEEE Trans. Pattern Analysis Machine Intelligence* **11**, pp. 674–693, 1989.
14. D. Colella and C. Heil, "The characterization of continuous, four coefficient scaling functions and wavelets," *IEEE Trans. Info. Theory* **38**, pp. 876–881, 1992.
15. M. J. Lai and D. Roach, "Construction of bivariate symmetric orthonormal wavelets with short support," *Under preparation* , 1999.